View Online

Fluorine-labeling as a diagnostic for thiol-ligand and gold nanocluster self-assembly†

Arthur W. Snow,* Edward E. Foos, Melissa M. Coble, Glenn G. Jernigan and Mario G. Ancona

Received 1st April 2009, Accepted 26th June 2009
First published as an Advance Article on the web 10th July 2009
DOI: 10.1039/b906510p

An ω-fluorine-labeled oxyethylene thiol ligand, $F(CH_2CH_2O)_2CH_2CH_2SH$, was synthesized, characterized and incorporated into mixed self-assembled monolayers with $CH_3(OCH_2CH_2)_3SH$ onto a planar gold substrate and onto 2 nm gold nanoclusters. The fluorine-labeled nanocluster was self-assembled onto gold substrates using alkane dithiol ($HS(CH_2)_nSH$; n = 5, 8, 11) and oxyethylene dithiol ($HS(CH_2CH_2O)_nCH_2CH_2SH$; n = 1, 2, 3) linking agents with equivalent chain lengths for comparative purposes. X-ray photoelectron spectroscopy (XPS) was used to track the fluorine-label in the self-assembly operations and to evaluate the effectiveness of the dithiols. For adequate XPS sensitivity at least 10% of the monolayer-forming molecules should be functionalized with this fluorine-label. In the comparative self-assembly of the fluorine-labeled gold nanoclusters in chloroform solution, the alkane dithiols were observed to be the more effective linking agents. This effectiveness correlates with the XPS analysis of alkane dithiols self-assembling onto the gold substrates with a higher packing density and with a larger fraction of molecules having one thiol group as opposed to two bonded to the gold surface. The oxyethylene dithiols self-assemble with a smaller packing density and a smaller fraction of molecules with an unbonded thiol group available for self-assembly.

Published on 10 July 2009 on http://pubs.rsc.org | doi:10.1039/B906510P
Downloaded by Naval Research Laboratory - Washington on 09 November 2010

Introduction

Fluorine-labeling of ligand-stabilized metal nanoclusters may serve as a useful analytical diagnostic for the effectiveness of procedures used to self-assemble such nanoparticles onto surfaces. Facile diagnostics for self-assembly procedures have important roles to play in the transition of this methodology to a materials and device fabrication technology. The graduation of self-assembly from a scientific endeavor to a manufacturing technology has been assessed as having feasibility but is reported to be difficult to evaluate due to the lack of experimental demonstrations of many key underlying concepts.[1] The underlying conceptions come from new-knowledge-seeking science for which the self-assembly literature is replete with many excellent reviews,[2] but the engineering of demonstrations with a sufficient level of control and replication over the number density and orientation of molecules and/or nanoparticles on a large scale along with attendant characterization have yet to be achieved.[1] The development of diagnostics that can provide such characterization and that can be adapted to large areal sizes would be an important step in fielding engineering demonstrations. The most widely utilized diagnostics for the assembly of nanoparticles in two- and three-dimensional arrays are images from scanning and transmission electron microscopies (SEM and TEM)[2–9] and proximal probe microscopies (STM and AFM).[8–11] While this characterization is excellent for isolated nanoscale detail, it does not integrate well over large surface areas (*e.g.* μm^2 or mm^2). The development of additional characterization tools for analysis of self-assembled depositions has been identified as a significant opportunity for future fundamental research as well.[2h] Additional tools used to investigate gold nanoparticle depositions include electronic absorption spectroscopy,[2e,3,5,7,8,9,12] optical reflectometry,[13] spectroscopic ellipsometry,[4,9,11,14] contact angle goniometry[9] and X-ray photoelectron spectroscopy (XPS).[7] Of these, only absorption spectroscopy is capable of quantifying a surface deposition without being cumbersome, time-consuming and expensive, but a transparent substrate is required. The next simplest and most informative technique is XPS. To characterize a number density of self-assembled nanoparticles on an opaque substrate, a particular element, which is not a constituent of the substrate or a ubiquitous contaminant and which has preferably a high sensitivity factor is needed. It is in this context that we hypothesize that a fluorine atom substituted into the structure of a few monolayer-forming molecules might be sufficient to act as a label to quantify the density of the deposition as detected by the XPS spectrum without perturbing the chemistry of the monolayer.

The objective of the present work is to design and demonstrate a fluorine-labeled organic thiol ligand that can be employed to provide analytical information about its self-assembly and about the self-assembly of labeled metal nanoclusters onto substrate surfaces. The future utility of such a diagnostic resides not only in information about the reproducibility of self-assembled nanostructures on a large scale but also in its use for the development of self-assembly procedures (*e.g.* selection of cluster linking agents and deposition conditions).

In this work a fluorine-labeled thiol ligand is synthesized, characterized, examined for XPS sensitivity in a diluted self-assembled monolayer and substituted by ligand exchange onto

Naval Research Laboratory, Washington, DC, 20375, USA. E-mail: arthur.snow@nrl.navy.mil

† Electronic supplementary information (ESI) available: Characterization of the fluorine-labeled ligand. See DOI: 10.1039/b906510p

 This journal is © The Royal Society of Chemistry 2009

Report Documentation Page

Form Approved
OMB No. 0704-0188

Public reporting burden for the collection of information is estimated to average 1 hour per response, including the time for reviewing instructions, searching existing data sources, gathering and maintaining the data needed, and completing and reviewing the collection of information. Send comments regarding this burden estimate or any other aspect of this collection of information, including suggestions for reducing this burden, to Washington Headquarters Services, Directorate for Information Operations and Reports, 1215 Jefferson Davis Highway, Suite 1204, Arlington VA 22202-4302. Respondents should be aware that notwithstanding any other provision of law, no person shall be subject to a penalty for failing to comply with a collection of information if it does not display a currently valid OMB control number.

1. REPORT DATE	2. REPORT TYPE	3. DATES COVERED
APR 2009		**00-00-2009 to 00-00-2009**

4. TITLE AND SUBTITLE	5a. CONTRACT NUMBER
Fluorine-labeling as a diagnostic for thiol-ligand and gold nanocluster self-assembly	5b. GRANT NUMBER
	5c. PROGRAM ELEMENT NUMBER
6. AUTHOR(S)	5d. PROJECT NUMBER
	5e. TASK NUMBER
	5f. WORK UNIT NUMBER
7. PERFORMING ORGANIZATION NAME(S) AND ADDRESS(ES) **Naval Research Laboratory,4555 Overlook Avenue SW,Washington,DC,20375**	8. PERFORMING ORGANIZATION REPORT NUMBER
9. SPONSORING/MONITORING AGENCY NAME(S) AND ADDRESS(ES)	10. SPONSOR/MONITOR'S ACRONYM(S)
	11. SPONSOR/MONITOR'S REPORT NUMBER(S)

12. DISTRIBUTION/AVAILABILITY STATEMENT
Approved for public release; distribution unlimited

13. SUPPLEMENTARY NOTES

14. ABSTRACT

15. SUBJECT TERMS

16. SECURITY CLASSIFICATION OF:			17. LIMITATION OF ABSTRACT	18. NUMBER OF PAGES	19a. NAME OF RESPONSIBLE PERSON
a. REPORT	b. ABSTRACT	c. THIS PAGE			
unclassified	**unclassified**	**unclassified**	**Same as Report (SAR)**	**12**	

View Online

Downloaded by Naval Research Laboratory - Washington on 09 November 2010
Published on 10 July 2009 on http://pubs.rsc.org | doi:10.1039/B906510P

gold nanoclusters. These fluorine-labeled gold nanoclusters are used to assess the effectiveness of a series of dithiol coupling agents with different chain structures and chain lengths for self-assembly of the gold nanoclusters onto a gold surface. The result of this coupling agent experiment is counterintuitive to expectations for the effects of dithiol chain structure and chain length.

Results

Fluorine-labeled ligand

The structure of the fluorine-labeled thiol ligand consists of a single fluorine substituent at the end of an oxyethylene chain as depicted in Fig. 1. This $F(CH_2CH_2O)_2CH_2CH_2SH$ (**1**) structure was selected to mimic an unlabeled methoxy-terminated oxyethylene thiol, $CH_3(OCH_2CH_2)_3SH$ (**2**), which has been used as a stabilizing ligand for previous gold cluster work involving synthesis,[15] chemical sensors[16] and self-assembly.[17] The oxyethylene chain structure imparts solubility in both water and organic solvents for both the ligand and corresponding gold clusters which makes it a very versatile ligand for self-assembly operations. Its chain length of 10 atoms (excluding sulfur) is a good compromise in the thickness for a gold cluster ligand shell between stability against aggregation and electron transport between adjacent clusters. The absence of an ionic charge facilitates measurement and interpretation of electrical conductivity on ensembles of clusters. The fluorine-labeling in effect shortens the chain by one atom and replaces the methoxy group of **2** with a fluorine substituent but maintains the linear streamline structure. This does represent a perturbation in chain length and in polarity of the terminal group. There is no evidence that oxyethylene chains of this length have a tightly packed morphology in monolayers, thus the chain length effect should be nominal. The $-CH_2F$ group dipole moment (1.81 D) is a little larger than that of the $-CH_2OCH_3$ group (1.30 D),[18] so the concentration of the fluorine-label will contribute a small amount of additional polarity.

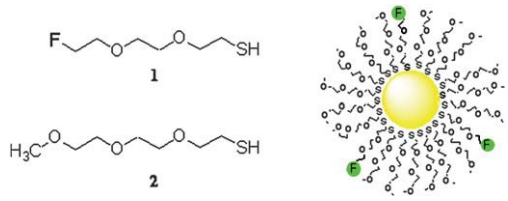

Fig. 1 Structures of fluorine-labeled oxyethylene thiol ligand (**1**) and methyl-terminated tri-ethoxyethylene thiol ligand (**2**) and a representation of the gold cluster labeled with the fluorine-substituted ligand.

The synthesis of the fluorine-labeled oxyethylene thiol ligand, **1**, was conducted by two routes as depicted in Fig. 2. Both routes start with triethylene glycol, **3**, and make use of alcohol-tosylate-thiol and alcohol-tosylate-fluoride transformations. The alcohol-tosylate-thiol conversion works well with the oxyethylene chain molecules[19–21] while the alcohol-tosylate-fluoride reaction sequence was adopted from reported successful conversions of alkyltosylates.[22,23] The statistical synthesis route consists of two steps. It converts the triethylene glycol, **3**, to the ditosylate, **4**, which then proceeds through a one-pot two-sequence step using stoichiometric quantities of tetrabutylammonium fluoride to displace half of the tosylate groups with the fluoride followed by addition of thiourea and subsequent hydrolysis of the adduct to convert the remaining tosylate groups to the thiol. The crude product is a statistical distribution of the fluorine-terminated oxyethylene thiol product, **1**, and dithiol- and difluoro-terminated oxyethylene byproducts. After chromatography, an overall 11% yield is obtained although a small amount of the difluoro-byproduct is difficult to completely separate. The sequential synthesis route takes advantage of a facile separation of the monotosylated triethylene glycol, **5**, from the triethylene glycol.[20] The tosylate is then displaced with fluorine to yield the fluorine-terminated triethylene glycol, **6**. This intermediate is tosylated to yield **7** which is then converted *via* thiourea and hydrolysis to the fluorine-terminated oxyethylene thiol product, **1**. Although four steps as opposed to two are required, the overall yield is 48%, and there are no symmetrical byproduct contaminants. This product and the intermediates were characterized by NMR and IR spectroscopies as well as elemental analysis (see Experimental and ESI†). The ^{19}F NMR spectrum of the fluorine terminated compounds displays a triplet of triplets at −223 ppm which is a characteristic signature of the $-CH_2CH_2F$ substructure,[24] and this spectrum readily detects any of the symmetrical bis(fluoro)-byproduct (from transformation of **4** to **1**) by a small but resolved chemical shift for this symmetrical contaminant.

Fluorine-labeled ligand monolayer – XPS sensitivity

To address the question of XPS sensitivity to the fluorine-labeled ligand in a monolayer assembly an experiment was conducted where varying quantities of **1** and **2** were co-mixed and self-assembled onto a gold surface. Fig. 3a depicts an XPS survey spectrum of a monolayer of **1** on a gold substrate. Peaks at binding energies of 285, 532, 686, 165 and 229 eV correspond to

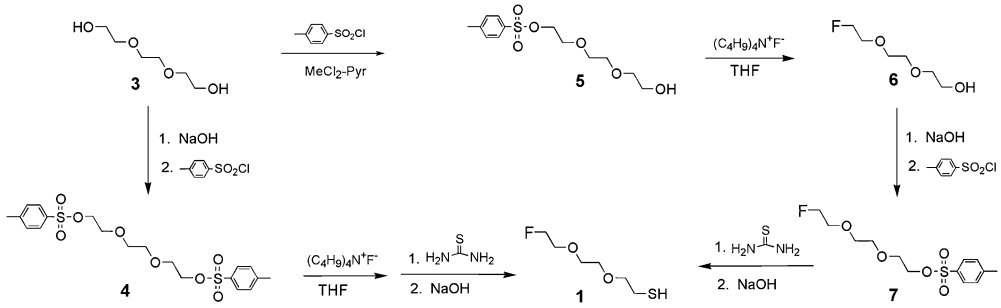

Fig. 2 Synthetic routes for synthesis of the fluorine-labeled oxyethylene thiol ligand (**1**).

View Online

Downloaded by Naval Research Laboratory - Washington on 09 November 2010
Published on 10 July 2009 on http://pubs.rsc.org | doi:10.1039/B906510P

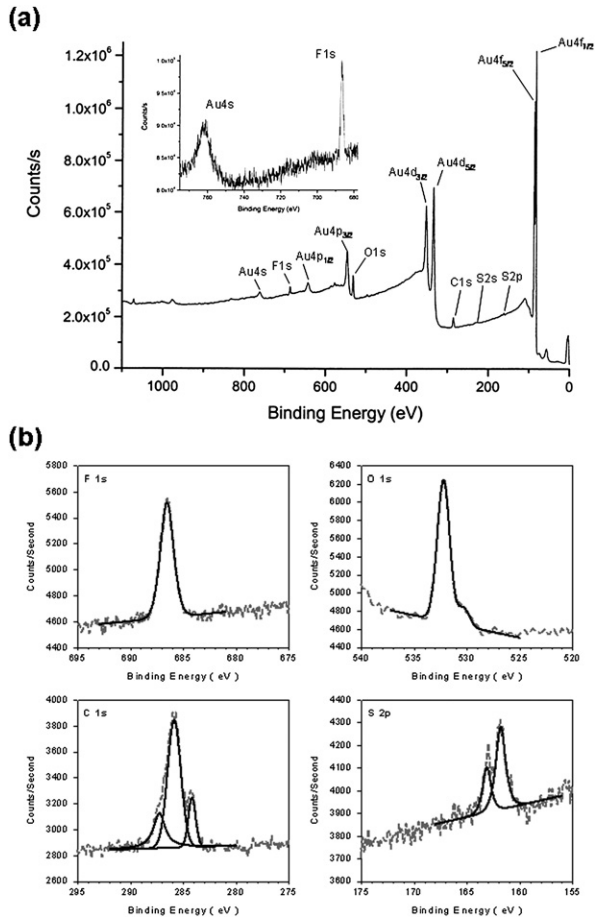

Fig. 3 (a) XPS survey spectrum of a self-assembled monolayer of **1** onto a gold surface. The inset is a high-resolution scan of the Au4s and F1s region. (b) XPS F1s, O1s, C1s and S2p high-resolution spectra of a self-assembled monolayer of **1** onto a gold surface. The experimental data in the spectra are represented by dots and the deconvoluted spectra by continuous lines.

the respective C1s, O1s, F1s, S2p and S2s emissions of the constituent elements. Fig. 3b presents the high-resolution spectra of these elements. Integration of high-resolution scans of the C1s, O1s, S2p and F1s regions yields a sensitivity factor corrected C:O:S:F area ratio of 6.4:2.6:1.2:1.0 which is consistent with the corresponding 6:2:1:1 stoichiometric composition ratio of **1**. The C1s in the high-resolution scan displays a distribution of binding energy peaks at 284.2, 285.8 and 287.2 eV in an intensity ratio that corresponds to 1 C–S: 4 C–O: 1 C–F bonded carbon atoms in the structure of **1**. This result was obtained by removal of carbon and oxygen contamination from the gold substrate surface by argon sputtering immediately prior to deposition of self-assembled **1**. When contamination is present, to obtain a good stoichiometric XPS analysis requires that the deposited monolayer displace carbon contamination from the substrate surface as has been previously deduced or assumed by earlier workers for analyses of monolayer composition.[25] Our efforts to obtain a good analysis utilizing only the chemical cleaning procedures described in the Experimental resulted in the observation of residual C and O contamination remaining on the Au surface. After self-assembled deposition of **1** on such contaminated surfaces, a significant excess of O (a factor up to 2.4) relative to its C:O:S:F composition remained although the relative compositions of C, S and F were consistent with the 6:2:1:1 stoichiometry.

Also depicted in Fig. 3a are emissions associated with the binding energies for gold atoms of the substrate. These Au emissions may be used as a reference to quantify the amount of fluorine present in the mixed monolayers of **1** and **2**. A series of mixed monolayers were self-assembled onto gold substrates from chloroform solutions. The percentage of the fluorine-labeled thiol, **1**, mixed with the unlabeled analog, **2**, varied from 100–50–20–10–5–2–1%, and the corresponding F1s emission gradually disappeared in the noise as the percentage of **1** fell below 10%. A plot of the F:Au ratio against the mole fraction of 1 in the self-assembly deposition mixture is shown in Fig. 4. Extrapolation to the x-intercept yields an XPS detection limit of 8 fluorine-labeled molecules per 100 in the monolayer, which assumes the monolayer composition reflects the relative concentrations of ligands in the solution from which it was deposited. This assumption seems reasonable based on the similar structure and solubility characteristics of **1** and **2**. Both are low viscosity liquids with relatively short chain lengths that would have little tendency to form highly ordered monolayers that might segregate on a surface. The plot is nonlinear which might reflect a kinetic difference for adsorption and bonding to the gold surface. The Au4s emission was used as the reference for the F:Au ratio on the basis of a similarity with the F1s emission intensity, binding energy – penetration depth and orbital symmetry factor recommended for calculating elemental ratios[26] (see inset of Fig 3). Using the Au4f7/2 emission yields a sensitivity plot with slightly more curvature but the same detection limit.

The series of mixed monolayers of **1** and **2** described above was further characterized by water contact angle measurements to assess differences in wetting (Fig. 5). As the composition varies from the 100% $–CH_2F$ terminated oxyethylene thiol to the 100% $–CH_2OCH_3$ terminated oxyethylene thiol, the contact angle increases from 67° to 73°. This 6° difference is small and correlates with the dipole moment difference associated with these structures indicated above. The slightly larger polarity of $–CH_2F$ terminal group in the monolayer is consistent with a modest

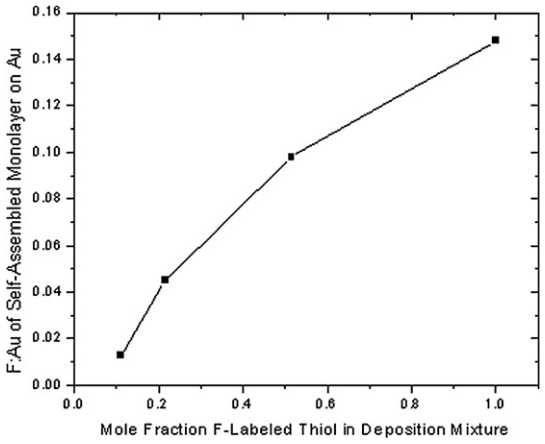

Fig. 4 XPS F:Au ratio as a function of monolayer composition of fluorine-labeled thiol (**1**) in methoxy-terminated thiol (**2**).

 This journal is © The Royal Society of Chemistry 2009

View Online

Downloaded by Naval Research Laboratory - Washington on 09 November 2010
Published on 10 July 2009 on http://pubs.rsc.org | doi:10.1039/B906510P

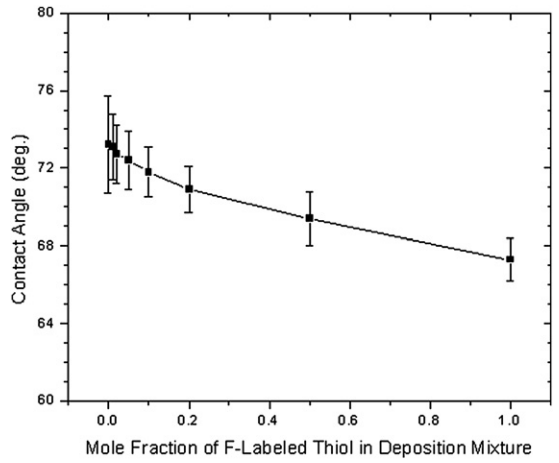

Fig. 5 Water contact angle as a function of monolayer composition of fluorine-labeled thiol (**1**) in methoxy-terminated thiol (**2**).

increase in wetting as this group predominates in the mixed monolayer.

Fluorine-labeled gold clusters

The fluorine-labeled gold cluster is depicted in Fig. 1. The objective in its preparation was to substitute a sufficient number of fluorine-labeled ligands onto the gold nanocluster such that they would be detectable in the XPS spectrum but that they have minimal effect on other properties. Using Fig. 4 as a guide for XPS sensitivity to fluorine in a mixed monolayer of **1** in **2**, a 30% degree of substitution was targeted for the fluorine-labeling. The precursor cluster had a 2 nm gold core stabilized by a shell composed of **2** and was prepared from a hexanethiol stabilized cluster as previously reported.[16] The fluorine-labeled cluster was prepared in a single-step ligand exchange reaction between the precursor cluster and free fluorine-labeled thiol **1** as reported in the Experimental. The degree of substitution was quantified by NMR analyses of displaced ligands after treatment with tetraethyl ammonium cyanide and was calculated at 29% from integration of the $-CH_2F$ and $-OCH_3$ terminal group resonances

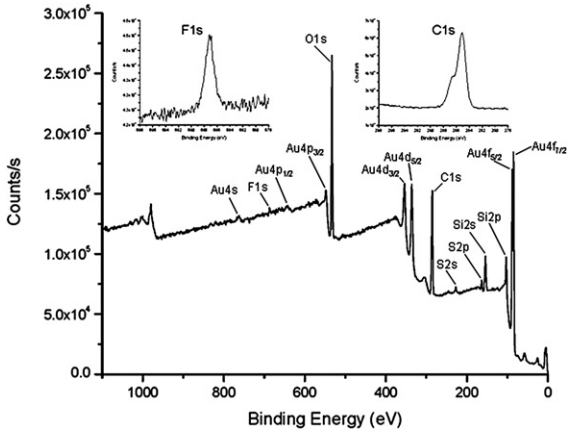

Fig. 6 XPS survey spectrum of a solution evaporated film of fluorine-labeled gold clusters supported on a SiO_2 surface. The insets are a high-resolution scans of the F1s and C1s regions.

of the displaced ligands. This cluster was characterized by NMR and IR spectroscopies (see ESI†) for comparison of spectral features with those of the free ligands). The ^1H NMR spectrum consisted of a broad resonance at 3–4 ppm corresponding to the oxyethylene protons and a broadened doublet at $\delta = 4.51$ ppm corresponding to the terminal $-CH_2F$ group. There is a correspondence in chemical shifts of these broad resonances from the cluster with the sharp ones from the free thiol ligands as depicted in the ESI.† The ^{19}F NMR spectrum of the fluorine-labeled cluster displays a broad resonance at -222.6 ppm which has an analogous correspondence with that of the free thiol triplet of triplets at $\delta = -223.30$ as is also depicted in the ESI.† An XPS spectrum of this cluster (see Fig. 6) was obtained from a film deposited on SiO_2 by evaporation of a droplet of the cluster in chloroform solution. The F1s peak was observed at 687 eV, and the C1s peak was observed at 285 eV with partially resolved shoulder at ~287 eV characteristic of the terminal $-CH_2F$ structure in the labeled thiol. This batch of fluorine-labeled nanocluster was used in all subsequent experiments involving its self-assembly onto gold substrates with various dithiols.

Self-assembly of fluorine-labeled gold clusters

The following gold nanocluster self-assembly experiment was designed to use the fluorine-label as a diagnostic for the effectiveness of two series of α,ω-dithiols to serve as linking agents between a gold substrate and the gold cluster stabilized by the oxyethylene thiol ligand shell. The two series of α,ω-dithiols consist of alkane chains and oxyethylene chains with chain lengths of 5, 8 and 11 atoms between the thiol functional groups. These dithiols are depicted in Table 1, and a representation of the self-assembly is illustrated in Fig. 7. There are two hypotheses to be tested by these series. The first concerns the effect of chain length. A reasonable expectation would be that dithiols of longer chain length would be more effective in penetrating a nanocluster ligand shell to displace a monothiol from the gold core surface while at the same time being bonded to the gold substrate by the other thiol group. In previous work on multilayered self-assemblies of gold nanoclusters with alkanedithiols of chain lengths ranging from 6 to 12 methylene groups this expectation appeared to be consistent with the longer chain dithiols being more effective in promoting the

Table 1 XPS analysis[a] of self-assembled fluorine-labeled nanoclusters

Dithiol linking agents	F:Au	F:C	C:Au
alkane dithiols			
$HS(CH_2)_5SH$	0.051	0.037	1.37
$HS(CH_2)_8SH$	0.037	0.032	1.14
$HS(CH_2)_{11}SH$	0.046	0.025	1.87
oxyethylene dithiols			
$HS(CH_2CH_2O)_1CH_2CH_2SH$	0.029	0.032	0.91
$HS(CH_2CH_2O)_2CH_2CH_2SH$	0.030	0.031	0.97
$HS(CH_2CH_2O)_3CH_2CH_2SH$	0.022	0.020	1.12
control experiments			
no dithiol in first step	0.054	0.054	1.00
monothiol **2** in first step	0.005	0.008	0.64

[a] The precision of the XPS measurements is an estimated ±5% and the ratios are corrected for element sensitivity factors.

View Online

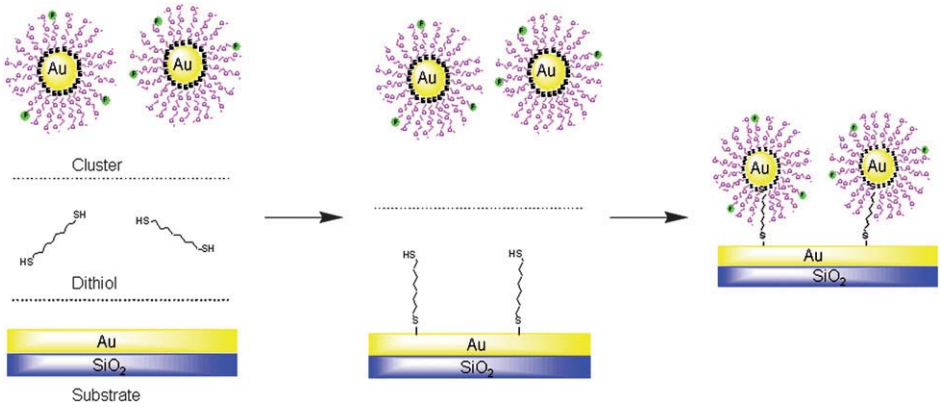

Fig. 7 Representation of the two step procedure for self-assembly of fluorine-labeled gold nanoclusters to a gold surface with dithiol linking agents.

Downloaded by Naval Research Laboratory - Washington on 09 November 2010
Published on 10 July 2009 on http://pubs.rsc.org | doi:10.1039/B906510P

self-assembly.[27] The diagnostic in this previous work was an electrical conductivity increase with increasing numbers of cluster depositions, and, when the dithiol passed a threshold chain length, electrical conductivity of the ensemble was no longer a valid diagnostic of self-assembly efficiency. The second hypothesis addresses the effect of chain structure. In this case the expectation is that an oxyethylene dithiol in comparison with an alkanedithiol would have more chemical compatibility with the oxyethylene thiol ligands of the nanocluster shell. This would have a more facile diffusion through the ligand shell to the gold core and thus promote a more effective linking of the nanocluster to the gold substrate. While not examined here, the role of the solvent in expanding the hydrodynamic volume of the ligand shell and promoting diffusion through it could affect the two systems differently.

For each of the six dithiols the self-assembly procedure as represented in Fig. 7 involved a two step treatment of a gold substrate with dithiol and fluorine-labeled cluster solutions. The freshly cleaned gold substrate was successively immersed 15 min in a 1% solution of dithiol in chloroform then immersed 15 min in a 0.5% solution of the fluorine-labeled clusters in chloroform. The 15 min immersion times were selected for two reasons. This deposition condition had been used previously with success in the preparation of multilayer films of clusters,[17,27] and a relatively short immersion time is more likely to discriminate a rapid effective self-assembly process from a slow one.

These self-assembled preparations were analyzed by XPS for the F:Au, F:C and C:Au composition ratios as determined from integration of the F1s, Au4f7/2 and C1s peaks. The results are presented in Table 1. These ratios correlate with quantity of clusters deposited on the Au substrate and with the type of dithiol coupling agent used: the source of the fluorine being the clusters alone *via* the labels attached to their shells; the source of the gold being either the cluster's core or the substrate; and the source of the carbon being the thiol ligands of the cluster's shell and the dithiol coupling agent used. The F:Au ratios for the alkane dithiol system are all larger than those for the oxyethylene dithiol system. The indication is that more of the fluorine-labeled clusters are bonded to the gold surface by the alkane dithiol system. This result appears to be independent of chain length in either system. The C:Au ratios for the alkane dithiol system exceed those for the oxyethylene system. This result is also consistent with the alkane dithiol system bonding a larger number of nanoclusters to the gold surface than does the oxyethylene dithiol system although there may be some contribution from the alkane dithiol coupling agent which is more carbon rich than the oxyethylene dithiol coupling agent. The F:C ratio does not reflect a significant difference between the alkane dithiol and oxyethylene dithiol systems, but within each system there appears to be a small diminishing trend with increasing chain length of the dithiol. For the clusters alone this ratio should be constant, however, with the dithiol coupling agents present on the Au substrate surface, their contribution to the F:C ratio has the effect of diminishing it as the dithiol chain lengthens. This effect is small as depicted in Table 1.

Overall, within each dithiol system, the composition ratios do not appear to reflect a significant or regular dependence on chain length of the dithiol as reflected mainly by the F:Au ratio and to some extent the C:Au ratio. These results are not what were anticipated according to the two hypotheses described above. In seeking additional information, two control experiments were conducted to assess the effects of nonspecific adsorption of the nanoclusters. In the first, the dithiol compound was simply eliminated from the self-assembly procedure, and a direct observation of non-specific adsorption of the cluster was made. The F:Au ratio of 0.054 for this control experiment is significant as it equivalent or greater that the F:Au values for the other experiments where dithiols were employed. This observation clearly indicates the presence of active sites in the freshly cleaned Au substrate that can adsorb the oxyethylene thiol stabilized cluster without the dithiol serving to make a linkage between cluster and substrate. Although not often discussed in the literature, such observations have been made with regard to both SiO_2 and Au surfaces.[17d,27] While the nature of such active sites is not understood, when these sites are passivated, the non-specific adsorption is diminished and the nanocluster adsorption can be attributed to the dithiol. This is demonstrated in the second control experiment where the oxyethylene monothiol **2** is used in place of the dithiol in the two-step self-assembly. The non-specific adsorption diminishes to one tenth of its initial value. Thus, the dithiols in Table 1 can similarly passivate the non-specific active sites and be responsible for the cluster adsorption.

 This journal is © The Royal Society of Chemistry 2009

View Online

Downloaded by Naval Research Laboratory - Washington on 09 November 2010
Published on 10 July 2009 on http://pubs.rsc.org | doi:10.1039/B906510P

Discussion

Self-assembled dithiol molecular packing and surface bonding

The self-assembly results in Table 1 lead to a questioning of the extent of formation of the monolayer and to the nature of its morphology when the dithiols are adsorbed on the gold substrate surface. The self-assembly of α,ω-alkanedithiols onto clean gold surfaces has been studied. With some dependence on chain length, alkanedithiol monolayers have been reported to bond to planar gold surfaces with one or both thiol groups and to orient in an upright, flat or looped positions.[28] In the absence of a good study of a homologous series of alkanedithiol monolayers, the trend indicated by this literature appears to be: (1) short chain length dithiols (*e.g.* hexanedithiol) form well ordered monolayers where both thiol groups bond to the surface and the chain is parallel to the surface;[28h] (2) intermediate chain length dithiols (*e.g.* octanedithiol, nonanedithiol) form monolayers where thiol group bonding and chain orientation are similar to that of the short chain dithiols[28c,d,e,f,l,m] and/or where one thiol group bonds to the surface and the chain is oriented upright to the surface with the second thiol group projecting outward;[28b,g,i,l,m] (3) long chain length dithiols (*e.g.* dodecanedithiol) in some cases form less ordered monolayers where the bonding involves both thiol groups with the chain in a looped conformation[28g,j] and in other cases form more ordered monolayer structures with a single thiol group bonded to the substrate and the chain extending outward.[28a] The foregoing makes it difficult to assess the availability of an alkanedithiol's ω-thiol group for linking to a nanocluster while the α-thiol group is bonded to a planar substrate. Ideally, the ω-thiol group would be at the outer surface of a loosely packed amorphous monolayer and on a long enough tether so that diffusion of this ω-thiol group through the shell of an incoming cluster to form a bond with the core would be a facile process. If both thiol groups are bonded to substrate atoms as indicated for short chain dithiols above, then the dithiol's ability to participate in self-assembly would require that one of the S–Au bonds have a dynamic nature (rapid dissociation and reformation). As the dithiol chain lengthens to an intermediate size, the kinetics and thermodynamics are less favorable toward loop formation with the substrate surface, and the dithiol monolayer might be envisioned as an amorphous mixture of looped and tethered molecules loosely packed on the surface. An interesting morphology has been proposed from AFM images for the 1,8-octanedithiol on Au system where isolated protrusions of single thiolate attached "standing molecules" are interspersed in a film of predominantly "lying down molecules" with both thiolate groups bonded to the Au surface.[28m] Such a coupling agent morphology could be consistent with a subsequent deposition of low density of cluster. Graduating from intermediate to long dithiol chain lengths, lateral interactions between adjacent chains in a self-assembled monolayer deposition become significantly stronger, and a dense packing of extended chains with the 30° tilt angle from a surface normal characteristic of a monofunctional alkanethiol can result. The transition from an amorphous loosely packed monolayer to a densely packed extended chain morphology at a threshold chain length of 10 or greater methylene groups is classic behavior for monofunctional alkanethiols and is attributable to the van der Waals lateral interactions between the long methylene chains to promote the densely packed crystalline morphology.[29] Some reports of insertion of α,ω-alkanedithiols into pre-formed self-assembled monolayers of monofunctional alkanethiols claim that the dithiol is bonded to the gold surface in an upright orientation with a free thiol group extending outward.[30] The claim is supported primarily by STM and AFM images and does not quantitatively address the degree of dithiol-monothiol exchange or large areas of the substrate.

With regard to oxyethylene dithiols, comparable work characterizing their self-assembled monolayer formation and its morphology has not been reported. However, significant work has been reported for oxyethylene monothiols[31] and for alkane thiols terminated with short[32] and long[33] oxyethylene chains. For self-assembled monolayers in the oxyethylene thiol series, $HS(CH_2CH_2O)_nCH_3$, n = 3, 4, 5, 6, a transition occurs from a disordered amorphous morphology to an ordered morphology of oxyethylene chains in helical conformations at chain lengths of $n \geq 5$.[31] For oxyethylene chains as a terminal segment on an alkanethiol in a self-assembled monolayer, the shorter oxyethylene chain lengths tend to be amorphous or liquid-like although a crystalline packing can be achieved if the alkane chain part of the molecule is long enough to form a close packed crystalline base that can induce order into the oxyethylene segments in the terminal groups.[2h,32] The oxyethylene chain itself is more flexible than an alkane chain and much less likely to crystallize. As such, the oxyethylene dithiols with a lower tendency toward crystalline packing could have a greater tendency to orient in a horizontal or looped position on the Au substrate. This might explain their lower effectiveness to form linkages between the substrate and clusters in solution as reflected by the comparative F:Au ratios in Table 1.

In considering the oxyethylene- and alkanedithiol self-assembled depositions alone on a gold surface, the XPS measurements of the C:Au ratios for the six dithiols (Table 2) appear to offer some insight. With the exception of the $HS(CH_2)_{11}SH$ deposition, the value of this ratio is very similar for the three oxyethylene dithiols and other two alkane dithiols. The C:Au ratio of 1.21 for the undecanedithiol is twice that of the other dithiols and initially appeared to be anomalous. However, with respect to the alkanethiol and α,ω-alkanedithiol systems discussed above, their chain length passes that

Table 2 XPS analysis[a] of C:Au ratio for dithiol self-assembled depositions

Dithiol linking agents	C:Au
alkane dithiols	
$HS(CH_2)_5SH$	0.60
$HS(CH_2)_8SH$	0.59
$HS(CH_2)_{11}SH$	1.21
oxyethylene dithiols	
$HS(CH_2CH_2O)_1CH_2CH_2SH$	0.59
$HS(CH_2CH_2O)_2CH_2CH_2SH$	0.63
$HS(CH_2CH_2O)_3CH_2CH_2SH$	0.68

[a] The precision of the XPS measurements is an estimated ±5% and the ratio corrected for element sensitivity factors.

View Online

Downloaded by Naval Research Laboratory - Washington on 09 November 2010
Published on 10 July 2009 on http://pubs.rsc.org | doi:10.1039/B906510P

threshold of 10 or more methylene groups where lateral interactions between adjacent alkanedithiols stabilize a closely packed monolayer, and at that threshold or longer the constituent molecules start to assume an extended chain conformation with one free thiol group oriented away from the surface. To interpret the data in Table 2 we speculate that the five dithiol depositions with the C:Au ratio in the 0.60 to 0.70 range are loosely packed with chains more parallel to the substrate surface while, the undecanedithiol deposition is more densely packed with a larger fraction of molecules in a more efficiently packed conformation (*e.g.* partial chain extension or conically shaped coil) and more oriented away from the substrate surface.

A more in-depth comparative analysis of the molecular packing density and thiol bonding was conducted on self-assembled depositions of fluorine-labeled monothiol **1**, and the 11-atom chain length oxyethylene- and alkanedithiols. This involved preparation of self-assembled samples of these thiol compounds on gold substrates that were treated with argon sputtering to remove carbon and oxygen contamination as described above and obtaining high resolution XPS S2p spectra (see Fig. 8). Previous XPS studies of alkanethiols on gold have shown that the S2p region consists of a doublet assigned to the S2p3/2 and S2p1/2 peaks separated by 1.2 eV with a 2:1 area ratio.[34] When the sulfur is bonded as a thiolate to gold, the S2p3/2 binding energy is at 162 eV, and, when the sulfur is present as a free thiol, the S2p3/2 binding energy is at 164 eV.[34] The spectra in Fig. 8 were analyzed using this doublet spectral shape and 2:1 area ratio to obtain an optimized fit for each of the three thiol compounds. The vertical dashed lines represent binding energy where the maximum occurred for the S2p3/2 peaks of the dithiol spectra. The areas of the S2p peaks are entered in Table 3, as is the area ratio of gold-bonded sulfur to free thiol (S2p(Au):S2p(H)). These ratios (7.4:1 for the oxyethylenedithiol and 4.8:1 for the alkanedithiol) indicate most of the sulfur of both dithiols in these self-assembled depositions is bonded to the gold surface although the number of free thiol groups is larger for the undecanedithiol. In the literature there are examples of measurement of these S2p(Au) and S2p(H) XPS peaks for determination of Au-bound and free thiol groups in self-assembled depositions.[28b,d,g,k] While not quantified into a ratio, three different studies[28b,g,k] of octanedithiol report very different results. Clearly, this characterization is dependent on deposition time, dithiol concentration, solvent used, substrate morphology and surface preparation treatment, *etc.*

In addition to assessing the relative amount of unbound thiol groups in a self-assembled dithiol deposition, the molecular packing or surface density of the dithiol on the gold surface is also an important factor in understanding the use of a dithiol as a coupling agent. Included in Table 3 are integrated areas of the Au4f7/2 substrate peak in the XPS spectrum and the S2p/Au4f7/2 area ratio. This S2p/Au4f7/2 area ratio has been used to characterize the packing density of alkanethiol compounds self-assembled on gold[35,36] and appears to be applicable here. The thickness of a self-assembled deposition and variations in elemental composition have attenuating effects on the Au peak intensity and need to be taken into account for determination of absolute numbers.[37] This attenuation of the Au peak intensity is

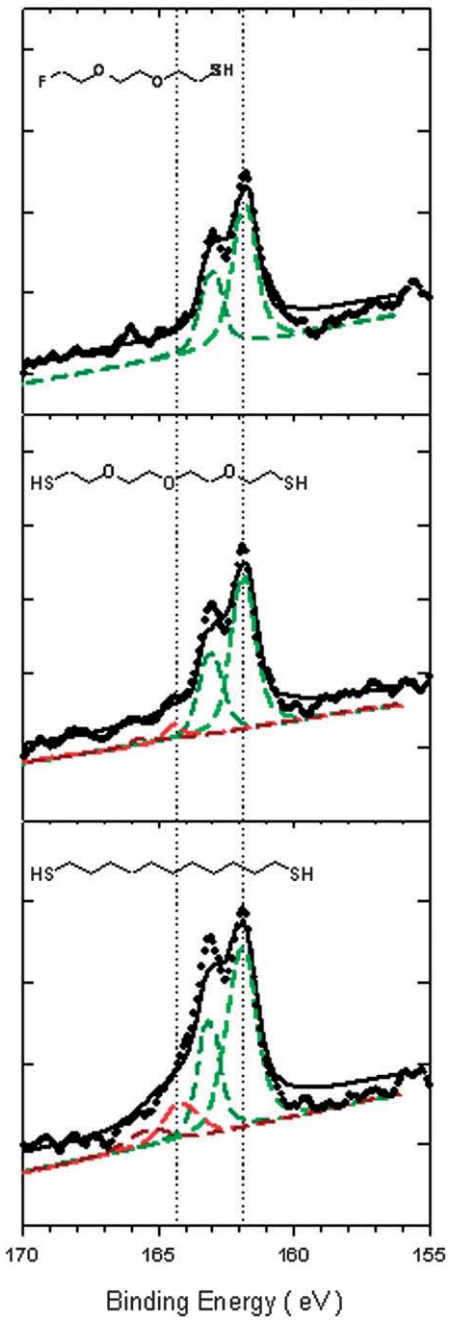

Fig. 8 High resolution XPS S2p spectra of self-assembled depositions of the fluorine labeled oxyethylene thiol **1**, and the $HS(CH_2CH_2O)_3CH_2CH_2SH$ and $HS(CH_2)_{11}SH$ dithiols. The spectra were deconvoluted by fitting the S2p doublets with a spin–orbit splitting of 1.2 eV and a 2:1 area ratio. In the case of the dithiols, the fit was conducted with two S2p doublets to obtain values for the relative quantity of Au-bound and free thiol. The raw XPS data (dots) have been deconvoluted to represent the S2p3/2 and S2p1/2 peaks (dashed lines) using a mix of Gaussian and Lorenzian line shapes and fit to a composite spectrum (solid line). The deconvoluted spectra of the individual S2p peaks are offset below the experimental baseline for clarity. Binding energies for the Au-bound S2p3/2 and unbound S2p1/2 peaks are161.9 eV and 164.2 eV respectively.

 This journal is © The Royal Society of Chemistry 2009

View Online

Table 3 XPS analysis[a] of the S2p peak intensity and deconvolution for the fluorine-labeled thiol **1** and the 11 atom length oxyethylene and alkane dithiols self-assembled films

	S2p(Au)		S2p(H)				
self-assemble films (thiol precursor)	161.9 eV (counts·eV)	163.1 eV (counts·eV)	164.2 eV (counts·eV)	165.4 eV (counts·eV)	S2p(Au):S2p(H) ratio	Au4f7/2 83.8eV (counts·eV)	S2p/Au4f7/2 ratio
$HS(CH_2CH_2O)_2CH_2CH_2F$	478	255	—	—	—	61096	0.0120
$HS(CH_2CH_2O)_3CH_2CH_2SH$	545	272	74	37	7.4	74838	0.0124
$HS(CH_2)_{11}SH$	739	369	152	76	4.8	55666	0.0240

[a] These measurements are an average of data taken from three different spots on the substrate and are not corrected for element sensitivity factors.

Published on 10 July 2009 on http://pubs.rsc.org | doi:10.1039/B906510P
Downloaded by Naval Research Laboratory - Washington on 09 November 2010

evident in Table 3 and is consistent with the undecanedithiol being the most densely packed or thickest deposition. Combined with a more intense S2p peak, the S2p/Au4f7/2 ratio is significantly larger for the undecanedithiol. Quantitatively, this ratio is a factor of two larger than that for the comparable oxyethylenedithiol (Table 3). Thus, the undecanedithiol, in addition to having a larger fraction of free thiol groups available for bonding to gold nanoparticles, also appears to have a higher packing density. This higher packing density correlates with a smaller conformation size for the undecanedithiol compared with that for an oxyethylenedithiol chain structure.[38] In a solvent such as chloroform where attractive interactions with the oxyethylene structure would be stronger those with the alkane chain, there would be an expectation of a larger hydrodynamic volume for an oxyethylene chain of sufficient length to coil. In the self-assembly process this larger volume would leave a less densely packed monomolecular layer after solvent evaporation.

Conclusion

Fluorine-labeling at the ω-position of an oligo-oxyethylene thiol ligand is a potentially useful diagnostic for the tracking of this thiol and of a metal nanocluster functionalized with this taggant in self-assembly operations. Synthesis of this fluorine-labeled ligand is readily accomplished using alcohol-tosylate-fluoride and alcohol-tosylate-thiol terminal group transformations. This molecule has very similar self-assembly properties to those of the non-labeled analogs and readily forms mixed monolayers. The sensitivity limit, when using XPS as the analytical diagnostic, requires incorporation of the fluorine-labeled molecule into the self-assembled entity at a degree of substitution of not less than 10% relative to the non-labeled molecular analogs.

With regard to using alkane- and oxyethylenedithiols as self-assembled depositions for coupling gold nanoparticles to gold substrates under the self-assembly conditions reported here, the alkanedithiols are more effective coupling agents irrespective of dithiol chain length. The alkanedithiol's higher packing density on the gold surface and their greater fraction of free thiol groups within the self-assembled deposition result in larger quantities of gold nanoparticles being self-assembled to the substrate. Of particular note is a two-fold greater dithiol packing density for the eleven atom alkanedithiol *versus* the oxyethylene dithiol analog.

Experimental

Materials

The following reagents were obtained from Aldrich: triethylene glycol (**3**), tetraethylene glycol, 1,5-pentanedithiol (**8**), 1,8-octanedithiol (**9**), 1,11-dibromoundecane, 2-mercaptoethyl ether (**11**), *p*-toluenesulfonyl chloride, tetrabutylammonium fluoride, 1.0 M THF (TBAF), sodium hydroxide, thiourea, magnesium sulfate, sodium chloride, sodium sulfate and lithium aluminum hydride, tetraethyl ammonium cyanide. 3,6,9-trioxodecane-1-thiol (**2**), 1,8-bis(tosyloxy)-3,6-dioxooctane (**4**) and 3,6-dioxooctane-1,8-dithiol (**12**) were prepared as reported in ref. 19. Solvents were obtained from Fisher Scientific and used as received unless otherwise specified.

Synthesis of *1-fluoro-3,6-dioxooctan-1-thiol* (1)

α-Fluoro-ω-tosyl triethylene glycol, **7**, (6.323 g, 20.64 mmol), thiourea (1.590 g, 20.89 mmol), ethanol (12.5 mL) and water (0.938 g) were added to a 50 mL round bottom flask fitted with a condenser, nitrogen inlet and stirring bar. The mixture was refluxed for 3 hr under nitrogen. A solution of NaOH (1.131 g, 28.27 mmol) in water (16.3 g) was added and the reflux continued for 4 hr. The reaction was worked up by concentrating at reduced pressure to a 20 mL volume to remove the ethanol, adding 5 mL water followed by dropwise addition of conc. HCl until mixture just becomes acidic. The mixture is extracted 2× with 25 ml methylene chloride, extracts are combined, dried over Na_2SO_4, filtered, concentrated at reduced pressure (50 °C/20 mm) and vacuum dried (23 °C/<1 mm) to yield 3.751 g of a light amber liquid crude product. The product was vacuum distilled (107–108 °C/7 mm) to yield a colorless liquid product (3.288 g, 95%). Anal. Calcd for $C_6H_{13}O_2SF$: C, 42.84; H, 7.79; S, 19.06; F, 11.29. Found: C, 42.81; H, 8.00; S, 19.13; F, 11.13. IR (neat): ν_{max}/cm^{-1} 2869, 2555, 1457, 1351, 1294, 1237, 1114, 1045, 935, 874 cm^{-1}. δ_H(300 MHz; $CDCl_3$; Me_4Si) 1.53 (t, $^3J_{HH} = 8$ Hz, 1H), 2.65 (q, 2H), 3.5–3.8 (m, 8H), 4.52 (d $^2J_{HF} = 46$ Hz of t $^3J_{HH} = 4$ Hz, 2H). δ_C(75 MHz; $CDCl_3$; Me_4Si) 24.16, 70.15, 70.22, 70.64, 72.82, 83.07. δ_F(282 MHz; $CDCl_3$; $CFCl_3$) −223.30 (t $^2J_{FH} = 48$ Hz of t $^3J_{FH} = 31$ Hz).

Synthesis of *8-tosyloxy-3,6-dioxooctan-1-ol* (5)

This compound was prepared by a slight modification of the procedure of Kuijpers.[20] Briefly, *p*-toluenesulfonyl chloride (7.50 g, 40.0 mmol) was added to a solution of triethylene glycol (60.0 g,

View Online

Downloaded by Naval Research Laboratory - Washington on 09 November 2010
Published on 10 July 2009 on http://pubs.rsc.org | doi:10.1039/B906510P

40.0 mmol) in pyridine (6.5 mL) and dichloromethane (400 mL) and under nitrogen. After stirring for 18 hr at room temperature, the solvent was concentrated under reduced pressure. The residue was dissolved in ethyl acetate (200 mL) and washed with aq. NaCl solution (3 × 200 mL). The aq. extract was back extracted with ethyl acetate (2 × 100 mL), and the combined ethyl acetate phases were dried over $MgSO_4$. After filtering and evaporating to dryness the product was purified on a silica column to yield a clear oil (9.30 g, 75%). IR (neat): ν_{max}/cm^{-1} 3421, 2886, 1594, 1358, 1169, 664. δ_H(300 MHz; $CDCl_3$; Me_4Si) 7.82 (d, $^3J_{HH}$ = 8.1 Hz, 2H), 7.36 (d, $^3J_{HH}$ = 8.1 Hz, 2H), 7.19 (t, $^3J_{HH}$ = 3.6 Hz, 2H), 3.59–3.78 (m, 10H), 2.47 (s, 3H). δ_C(75 MHz; $CDCl_3$; Me_4Si) 144.86, 132.93, 129.82, 127.96, 72.48, 70.77, 70.34, 69.13, 68.70, 61.74, 21.62.

Synthesis of *1-fluoro-3,6-dioxooctan-1-ol* (6)

A 3-neck 100 mL reaction flask was fitted with a dropping funnel, thermometer, stirring bar and nitrogen inlet and purged with dry nitrogen. The triethylene glycol monotosylate, **5**, (10.016 g, 32.9 mmol) was weighed into the reaction flask followed by pipette addition of dry THF (31.0 mL). After dissolution, TBAF (37. 0 mL 1.0 M/THF, 37.0 mmol) was transferred to the dropping funnel and added dropwise to the stirred reaction mixture. The reaction was stirred at 22 °C for 11 hr under N_2 and developed a dark brown coloration. The reaction was worked up by rotary evaporator concentration (50 °C/20 mm) to remove THF then vacuum distilled (105–115 °C/5 mm) to collect 3.58 g of an amber liquid. This crude product was redistilled (114–116 °C/4 mm) to yield 3.327 g (67% yield) of product as a colorless liquid. IR (neat): ν_{max}/cm^{-1} 3450, 2885, 1358, 1014 cm^{-1}. δ_H(300 MHz; $CDCl_3$; Me_4Si) 2.95 (s, 1H), 3.5–3.8 (m, 10H), 4.52 (d $^2J_{HF}$ = 51 Hz of t $^3J_{HH}$ = 4 Hz, 2H). δ_C(75 MHz; $CDCl_3$; Me_4Si) 61.54, 70.19, 70.38, 70.66, 72.45, 82.95. δ_F(282 MHz; $CDCl_3$; $CFCl_3$) −223.33 (t $^2J_{FH}$ = 48 Hz of t $^3J_{FH}$ = 31 Hz). CI MS: *m/z* 153 (MH^+).

Synthesis of *1-fluoro-8-tosyloxy-3,6-dioxooctane* (7)

To a 3-neck 50 mL reaction flask was fitted with a dropping funnel, thermometer, stirring bar and nitrogen inlet were added a solution of α-fluoro-ω-hydroxy triethylene glycol, **6**, (3.681 g, 24.2 mmol) in THF (7.4 mL) followed by a solution of NaOH (1.386 g, 34.6 mmol) in water (7.4 mL). The stirred reaction mixture was cooled to 5 °C. A solution of *p*-toluenesulfonyl chloride (4.603 g, 24.1 mmol) in dry THF (7.4 mL) was transferred to the dropping funnel and added dropwise under N_2 with rapid stirring and maintaining 5–8 °C over a 10 min period. The reaction continued for 4.5 hr at 5 °C and for an additional 1.5 hr as it warmed to room temperature. The two-phase reaction mixture was transferred to a sep funnel with addition of 10 mL diethyl ether, ether phase separated and aqueous phase extracted 3× with 10 mL quantities of ether. The combined ether extracts were back extracted with 10 mL quantities of water until neutral (pH paper) – 4 extractions needed. The ether phase was dried over anh Na_2SO_4, filtered, concentrated to dryness and vacuum dried (23 °C/<1 mm/12 hr) to yield a clear liquid (6.232 g, 85.3%). IR (neat): ν_{max}/cm^{-1} 2885, 1595, 1358, 1169, 1014, 640. δ_H(300 MHz; $CDCl_3$; Me_4Si) 2.40 (s, 3H), 3.5–3.8 (m, 8H), 4.12 (t $^3J_{HH}$ = 5 Hz, 2H), 4.51 (d $^2J_{HF}$ = 51 Hz of t $^3J_{HH}$ = 4 Hz, 2H), 7.32 (d, 2H), 7.78 (d, 2H). δ_C(75 MHz; $CDCl_3$; Me_4Si) 21.64, 68.72, 69.26, 70.57, 70.72, 70.76, 83.12, 127.97, 129.84, 132.92, 144.86. δ_F(282 MHz; $CDCl_3$; $CFCl_3$) −223.37 (t $^2J_{FH}$ = 51 Hz of t $^3J_{FH}$ = 31 Hz).

Synthesis of *1,11-undecanedithiol* (10)

This compound was prepared from the corresponding dibromide using a general procedure for conversion of an alkyl bromide to thiol *via* a thiourea adduct[39] adapted to α,ω-dibromoalkanes.[27] To a 50 mL reaction flask fitted with a condenser, nitrogen inlet and stirring bar were added 1,11-dibromoundecane (3.03 g, 9.65 mmol), thiourea (1.45 g, 19.04 mmol), ethanol (7 mL) and water (0.4 mL). After purging with nitrogen for several minutes, the mixture was refluxed for 3 hr after which a solution of NaOH (1.05 g, 26.2 mmol) in water (9.0 mL) was added and the reflux continued for 3 additional hr. On cooling a small quantity of oil formed and was separated. The aqueous phase was concentrated, neutralized by dropwise addition of conc. HCl and extracted 2× with methylene chloride. The extracts were combined with the oil, back extracted 2× with water, dried over $MgSO_4$, filtered and evaporated to dryness and vacuum dried (20 °C/1 mm) to yield a clear liquid (0.9786 g, 47%). mp −4 °C (lit. −5.4°C[40]). n_D^{22} 1.4933 (lit. 1.4931[40]). IR (neat): ν_{max}/cm^{-1} 2929, 2848, 2554, 1460, 1273, 724. δ_H(300 MHz; $CDCl_3$; Me_4Si) 1.2–1.4 (br, 8H; includes S–H triplet at 1.28), 1.56 (p, 2H), 2.47 (q, 2H). δ_C(75 MHz; $CDCl_3$; Me_4Si) 24.6, 28.3, 29.0, 29.4, 34.0.

Synthesis of *3,6,9-trioxooctane-1,11-dithiol* (13)

This compound was prepared from tetraethylene glycol by a procedure analogous to that for the preparation of **12**.[19] Briefly, the ditosylate of tetraethylene glycol intermediate was prepared by reacting a mixture of tetraethylene glycol (1.8590 g, 9.57 mmol) in THF (5 mL) and NaOH (1.1790 g, 29.5 mmol) in water (5 mL) with a solution of p-toluenesulfonyl chloride (3.6489 g, 19.1 mmol) in dry THF (5 mL) affording a crystalline product (3.8516 g, 80%). This intermediate (3.8516, 7.66 mmol) was then reacted with thiourea (1.1650 g, 15.3 mmol) in ethanol (10 mL) solution followed by addition of NaOH (0.7790 g, 19.5 mmol) in water (2 mL). The crude product was distilled (115 °C/1 mm) to yield the trioxyethylene dithiol product (0.8448 g, 40%). IR (neat): ν_{max}/cm^{-1} 2866, 2556, 1103 cm^{-1}. δ_H(300 MHz; $CDCl_3$; Me_4Si) 1.60 (t, 1H), 2.71 (q, 2H), 3.67 (m, 6H). δ_C(75 MHz; $CDCl_3$; Me_4Si) 24.2, 70.2, 70.5, 72.8.

Preparation of self-assembled mixed monolayer of 1 and 2 on gold

Substrates consisted of gold (500 Å) and chromium (50 Å) layers evaporated onto a silicon wafer which were cut into pieces of approximately 4 mm width by 20 mm length. These substrates were cleaned immediately before immersion in the self-assembly solution. The cleaning procedure consisted of successive 2 min immersions of the substrate in methylene chloride and 2-propanol followed by a UV-ozone treatment (Samco International, Inc., Model UV-1 UV-Ozone stripper/cleaner) of 12 min at 150 °C with a 0.50 L/min O_2 flow rate. The self-assembly of **1** and mixtures of **1** and **2** was conducted by immersion of the substrate

 This journal is © The Royal Society of Chemistry 2009

View Online

into a chloroform (HPLC grade) solution with a total thiol concentration of 10.0 mg thiol/g $CHCl_3$ solution and with the relative quantities of **1** and **2** varied for each particular monolayer preparation. The mole fraction of **1** in **2** was varied in the following series 1.00, 0.50, 0.20, 0.10, 0.05, 0.02, 0.01 of decreasing concentrations. The immersion times were 15 min after which substrates were rinsed in by two successive immersions in $CHCl_3$, then dried and stored in a desiccator. XPS analyses were conducted on the same day of preparation.

Preparation of fluorine-labeled gold clusters

The fluorine-labeled Au nanoclusters were prepared by a ligand substitution reaction where a precursor gold cluster having a 2 nm core and an oxyethylene thiol shell composed of **2**[16] undergoes a partial exchange of its unlabeled thiol ligands with the fluorine-labeled free thiol ligand **1**. To a 25 mL round-bottomed flask fitted with a N_2 inlet and a stirring bar, the oxyethylene precursor gold nanocluster (54.1 mg; corresponds to ~0.07 mmol of $-S(CH_2CH_2O)_3CH_3$ surface ligand) was dissolved in 5 mL CH_2Cl_2 followed by addition of **1** (9.8 mg; 0.06 mmol). This solution was stirred under N_2 for 15 h at 20 °C. The reaction was worked up by concentrating at reduced pressure to ~1 mL, precipitating by dropwise addition into 50 mL of stirred heptane and collecting by centrifugation (3000 rpm; 5 min). A second precipitation was conducted by redissolving the product in ~1 mL of CH_2Cl_2, reprecipitating into 50 mL of heptane and collecting by centrifugation followed by vacuum drying to yield 42.1 mg of product. IR (neat): ν_{max}/cm^{-1}) 2869, 1451, 1351, 1104, 1044, 874. δ_H(300 MHz; $CDCl_3$; Me_4Si) 3.38 (br), 3.66 (br), 4.55 (br d). δ_F(282 MHz; $CDCl_3$; $CFCl_3$) −222.6 (br). See ESI† for depiction of spectra.

Quantification of gold cluster ligand substitution

The composition of **1** and **2** in the cluster ligand shell was determined from NMR analyses of displaced ligands after a cyanide ion induced decomposition reaction in a procedure modified from one reported earlier.[41] In a 20 mL vial equipped with a stir bar, fluorine-labeled gold cluster product (18.4 mg; corresponds to ~0.02 mmol of surface ligand) was dissolved in approximately 5 mL of CH_2Cl_2 to form a deep red solution. The Et_4NCN (40.0 mg; 0.26 mmol) was dissolved in approximately 5 mL of CH_2Cl_2 and added to the vial, and the solution stirred at room temperature for 60 h. At this point the color had changed to a clear, golden yellow. The solution was concentrated to ~1mL and added dropwise to 60 mL of heptane producing a colorless supernatant and several drops of insoluble orange oil. The heptane was decanted and evaporated to yield a small quantity of colorless oil. ^1H NMR of this heptane soluble fraction was consistent with a mixture of $CH_3(OCH_2CH_2)_3S-$ and $F(CH_2CH_2O)_2(CH_2)_2S-$ moieties. A nanocluster encapsulating shell composition of 29% **1** and 71% $CH_3(OCH_2CH_2)_3S-$ was calculated from integration of the $-CH_3$ and $-CH_2F$ resonances.

Preparation of self-assembled thiol compounds for XPS analysis

Substrates consisted of gold (500 Å) and chromium (50 Å) layers evaporated onto a silicon wafer which were cut into pieces of approximately 4 mm width by 20 mm length. These substrates were treated by successive 2 min immersions in CH_2Cl_2 and 2-propanol followed by a UV-ozone treatment (Samco International, Inc., Model UV-1 UV-Ozone stripper/cleaner) of 12 min at 150 °C with a 0.50 L/min O_2 flow rate. They were then transferred to the XPS vacuum chamber and sputtered with argon until the carbon and oxygen contamination was no longer visible in the XPS. The cleaned substrates were removed from the vacuum chamber and immediately with minimal atmospheric exposure immersed in 10 mM solutions of the thiol compound in ethanol for 16 hr.

Instrumentation and analyses

NMR (^1H, ^{13}C, and ^{19}F) spectra were recorded on a Bruker Advance 300 NMR system operating at 300, 75.5, and 282 MHz, respectively. Spectra were referenced to TMS using the residual proton or carbon signal of $CDCl_3$ at δ 7.23 or 77.0 ppm, respectively, while ^{19}F NMR spectra were referenced to $CFCl_3$ internal standard at δ 0.0 ppm. FTIR spectra were recorded on a Nicolet Magna 750 FTIR spectrometer from thin film samples on a NaCl window. The −4 °C melting point of **10** was determined from the onset of a melting exotherm of a Differential Scanning Calorimetry thermogram recorded on a Du Pont Instruments TA 2100 and DSC 910. The refractive index of **10** was determined with a Bausch & Lomb ABBE-3L refractometer at the sodium D line (λ = 589 nm). Elemental analyses were performed by Schwarzkopf Microanalytical Laboratory.

Contact angle measurements were made using an ASC Products 2500 video contact angle system and software, from AST Products, Inc. VCA Version 1.90.0.9 which calculates the contact angle from 5 points on the image of the drop profile. A ~1 mm diameter droplet of triple distilled water was deposited onto a self-assembled monolayer coated substrate *via* syringe. The image was captured 10 sec after deposition and contact angle determined using the vendor software. Measurements on each sample were made in triplicate and error bar determined from the standard deviation.

XPS spectra were obtained with a monochromatic Al Kα X-ray source operating at 150 W with a spot size of ~500 μm. This large spot size was selected to avoid effect of microscopic inhomogeneities on the composition measurement of the self-assembled films. The precision of the XPS measurements is an estimated ±5%. The silicon wafer substrate samples were neutralized to the chamber ground potential through the use of Cu–Be clips of the sample holder. Pass energies were 100 eV for the survey scans, 46 eV for the F:Au composition of mixed monolayers and fluorine-labeled nanoclusters (Figs. 3a, 4, 6 and Table 1) and for the C:Au composition self-assembled dithiols (Table 2), and 20 eV for the high-resolution scans (Figs. 3b, 8, and Table 3). All spectra were collected at a takeoff angle of 90°. The binding energies were referenced to Au4f7/2 peak (84.0 eV). Samples were analyzed on the same day as their preparation. This is an important procedural point as illustrated using the octanedithiol for self-assembly with the fluorine-labeled gold clusters. Storage of the same samples under ambient conditions for eight days resulted F:Au, F:C and C:Au ratios of 0.029, 0.024 and 1.20 respectively which compare with 0.037, 0.032 and 1.14 (See Table 1) while the octanedithiol

Downloaded by Naval Research Laboratory - Washington on 09 November 2010
Published on 10 July 2009 on http://pubs.rsc.org | doi:10.1039/B906510P

View Online

self-assembly alone after eight days storage maintained an C:Au ratio of 0.59 unchanged from the value measured on the same day of preparation (See Table 2). For the XPS S2p analyses standard curve fitting software (PHI Multipak) employing a combination Gaussian and Lorenzian profiles was used to obtain a best fit. The model for fitting employs constraints of the S2p doublet having a 2:1 S2p3/2:S2p1/2 area ratio and a 1.2 eV splitting. The binding energy maxima of the S2p3/2 peak of these doublets occurs at 161.9 and 164.2 eV for the respective gold-thiolate and unbound thiol sulfur emissions as first described by Castner.[34]

Acknowledgements

The Office of Naval Research is gratefully acknowledged for financial support. The NRL Student Temporary Employment Program is also acknowledged by MMC for financial support. Prof. James E. Whitten of University of Massachusetts, Lowell is very appreciatively acknowledged for helpful discussion and suggestions.

Downloaded by Naval Research Laboratory - Washington on 09 November 2010
Published on 10 July 2009 on http://pubs.rsc.org | doi:10.1039/B906510P

References

1 Committee to Review the National Nanotechnology Initiative, National Research Council, *A Matter of Size: Triennial Review of the National Nanotechnology Initiative*, National Academy Press: Washington, D.C., 2006, (Chapter 5).
2 (*a*) A. Ulman, *Chem. Rev.*, 1996, **96**, 1533; (*b*) M. J. Hostetler and R. W. Murray, *Curr. Opin. Colloid. Interface Sci.*, 1997, **2**, 42; (*c*) A. N. Shipway, E. Katz and I. Wilner, *ChemPhysChem*, 2000, **1**, 18; (*d*) J. H. Fendler, *Chem. Mater.*, 2001, **13**, 3196; (*e*) M. Brust and C. J. Kiely, *Colloids and Surf.*, 2002, **202**, 175; (*f*) M.-C. Daniel and D. Astruc, *Chem. Rev.*, 2004, **104**, 293; (*g*) G. Schmid and U. Simon, *Chem. Commun.*, 2005, 697; (*h*) J. C. Love, L. A. Estroff, J. K. Kriebel, R. G. Nuzzo and G. M. Whitesides, *Chem. Rev.*, 2005, **105**, 1103; (*i*) B. L. V. Prasad, C. M. Sorensen and K. J. Klabunde, *Chem. Soc. Rev.*, 2008, **37**, 1871.
3 K. C. Grabar, P. C. Smith, M. D. Musick, J. A. Davis, D. G. Walter, M. A. Jackson, A. P. Gurthrie and M. J. Natan, *J. Am. Chem. Soc.*, 1996, **118**, 1148.
4 H. Wormeester, E. S. Kooij and B. Poelsema, *Phys. Rev. B*, 2003, **68**, 85406.
5 K. C. Grabar, R. G. Freeman, M. B. Hommer and M. J. Natan, *Anal. Chem.*, 1995, **67**, 735.
6 (*a*) V. Santhanam, J. Liu, R. Agarwal and R. P. Andres, *Langmuir*, 2003, **19**, 7881; (*b*) V. Santhanam and R. P. Andres, *Nano Lett.*, 2004, **4**, 41.
7 (*a*) Y. Joseph, I. Besnard, M. Rosenberger, B. Guse, H.-G. Nothofer, U. M. Wessels, U. Wild, A. Knop-Gericke, D. Su, R. Schlögl, A. Yasuda and T. Vossmeyer, *J. Phys. Chem. B*, 2003, **107**, 7406; (*b*) Y. Joseph, N. Krasteva, I. Besnard, B. Guse, M. Rosenberger, U. Wild, A. Knop-Gericke, R. Schlögl, R. Krustev, A. Yasuda and T. Vossmeyer, *Faraday Discuss.*, 2004, **125**, 77.
8 I. Hussain, Z. Wang, A. I. Cooper and M. Brust, *Langmuir*, 2006, **22**, 2938.
9 M. Wanunu, R. Popovitz-Biro, H. Cohen, A. Vaskevich and I. Rubinstein, *J. Am. Chem. Soc.*, 2005, **127**, 9207.
10 R. R. Bhat, D. A. Bischer and J. Benzer, *Langmuir*, 2002, **18**, 5640.
11 E. S. Kooij, H. Wormeester, E. A. M. Brouwer, E. van Broonhoven, A. van Silfhout and B. Poelsema, *Langmuir*, 2002, **18**, 4401.
12 M. Brust, D. Bethell, C. J. Kiely and D. J. Schiffrin, *Langmuir*, 1998, **14**, 5425.
13 E. A. M. Brouwer, E. S. Kooij, H. Wormeester and B. Poelsema, *Langmuir*, 2003, **19**, 8102.
14 R. R. Bhat and J. Genzer, *Surf. Sci.*, 2005, **596**, 187.
15 E. E. Foos, A. W. Snow and M. E. Twigg, *J. Cluster. Sci.*, 2002, **13**, 543.
16 E. E. Foos, A. W. Snow, M. E. Twigg and M. G. Ancona, *Chem. Mater.*, 2002, **14**, 2401.
17 (*a*) S. D. Jhaveri, D. A. Lowy, E. E. Foos, A. W. Snow, M. G. Ancona and L. M. Tender, *Chem. Commun.*, 2002, **14**, 1544; (*b*) M. G. Ancona, S. D. Jhaveri, D. A. Lowy, L. M. Tender, E. E. Foos and A. W. Snow, *Electrochimica Acta*, 2003, **48**, 4157; (*c*) S. D. Jhaveri, E. E. Foos, D. A. Lowy, E. L. Chang, A. W. Snow and M. G. Ancona, *Nano Lett.*, 2004, **4**, 737; (*d*) E. E. Foos, J. Congdon, A. W. Snow and M. G. Ancona, *Langmuir*, 2004, **20**, 10657.
18 A. Bondi, *Physical Properties of Molecular Crystal, Liquids, and Glasses*, John Wiley & Sons, Inc.: New York, 1968; p. 480.
19 A. W. Snow and E. E. Foos, *Synthesis*, 2003, **4**, 509.
20 W. H. A. Kuijpers and C. A. A. van Boeckel, *Tetrahedron*, 1993, **49**, 10931.
21 F. A. Loiseau, K. K. Hii and A. M. Hill, *J. Org. Chem.*, 2004, **69**, 639.
22 F. Nagatsugi, S. Sasaki and M. Maeda, *J. Fluorine Chem.*, 1992, **56**, 373.
23 M. S. Berridge and T. J. Tewson, *Appl. Radiat. Isot.*, 1986, **37**, 685.
24 E. F. Mooney, *An Introduction to 19F NMR Spectroscopy*, Heyden & Son, Inc.: London, 1970; p. 70.
25 (*a*) C. D. Bain, E. B. Troughton, Y.-T. Tao, J. Evall, G. M. Whitesides and R. G. Nuzzo, *J. Am. Chem. Soc.*, 1989, **111**, 321; (*b*) M. Buck, F. Eisert, J. Fischer, M. Grunze and F. Träger, *Appl. Phys. A*, 1991, **53**, 552; (*c*) T. Ishida, N. Nishida, S. Tsuneda and M. Hara, *Jpn. J. Appl. Phys.*, 1996, **35**, L1710.
26 B. D. Ratner and D. G. Castner, "Electron Spectroscopy for Chemical Analysis" in *Surface Analysis – The Principal Techniques*, ed. J. C. Vickerman, John Wiley & Sons; New York, 1997, (ch. 3), p. 62.
27 A. W. Snow, M. G. Ancona, W. Kruppa, G. G. Jernigan, E. E. Foos and D. Park, *J. Chem. Mater.*, 2002, **12**, 1222.
28 (*a*) T. Nakamura, H. Kondoh, M. Matsumoto and H. Nozoye, *Langmuir*, 1996, **12**, 5977; (*b*) H. Rieley, G. K. Kendall, F. W. Zemicael, T. L. Smith and S. Yang, *Langmuir*, 1998, **14**, 5147; (*c*) K. Kobayashi, J. Umemura, T. Horiuchi, H. Yamada and K. Matsushige, *Jpn. J. Appl. Phys.*, 1998, **37**, L297; (*d*) P. Kohli, K. K. Taylor, J. J. Harris and G. J. Blanchard, *J. Am. Chem. Soc.*, 1998, **120**, 11962; (*e*) K. Kobayashi, T. Horiuchi, H. Yamada and K. Matsushige, *Thin Solid Films*, 1998, **331**, 210; (*f*) K. Kobayashi, H. Yamada, T. Horiuchi and K. Matsushige, *Appl. Surf. Sci.*, 1999, **144–145**, 435; (*g*) C. Winter, U. Weckenmann, R. A. Fischer, J. Käshammer, V. Scheumann and S. Mittler, *Chem. Vap. Deposition*, 2000, **6**, 199; (*h*) T. Y. B. Leung, M. C. Gerstenberg, D. J. Lavrich and G. Scoles, *Langmuir*, 2000, **16**, 549; (*i*) W. Deng, D. Fujita, L. Yang, H. Nejo and C. Bai, *Jpn. J. Appl. Phys.*, 2000, **39**, L751; (*j*) A.-S. Duwez, G. Pfister-Guillouzo, J. Delhalle and J. Riga, *J. Phys. Chem. B*, 2000, **104**, 9029; (*k*) K. H. A. Lau, C. Huang, N. Yakovlev, Z. K. Chen and S. J. O'Shea, *Langmuir*, 2006, **22**, 2968; (*l*) J. Liang, L. G. Rosa and G. Scoles, *J. Phys. Chem. C*, 2007, **111**, 17275; (*m*) J.-J. Yu, J. N. Ngunjiri, A. T. Kelley and J. C. Garno, *Langmuir*, 2008, **24**, 11661.
29 M. D. Porter, T. B. Bright, D. L. Allara and C. E. D. Chidsey, *J. Am. Chem. Soc.*, 1987, **109**, 3559.
30 (*a*) S. Wakamatsu, J. Nakada, S. Fujii, U. Akiba and M. Fujihira, *Ultramicroscopy*, 2005, **105**, 26; (*b*) D. J. Fuchs and P. S. Weiss, *Nanotech.*, 2007, **18**, 1; (*c*) J.-J. Yu, J. N. Ngunjiri, A. T. Kelley and J. C. Garno, *Langmuir*, 2008, **24**, 11661.
31 D. J. Vanderah, J. Arsenault, H. La, R. S. Gates, V. Silin, C. W. Meuse and G. Valincius, *Langmuir*, 2003, **19**, 3752.
32 (*a*) C. Pale-Grosdemange, E. S. Simon, K. L. Prime and G. M. Whitesides, *J. Am. Chem. Soc.*, 1991, **113**, 12; (*b*) P. Hardner, M. Grunze, R. Dahint, G. M. Whitesides and P. E. Laibinis, *J. Phys. Chem. B*, 1998, **102**, 426; (*c*) S. Svedhem, C.-A. Hollander, J. Shi, P. Konradsson, B. Liedberg and S. C. T. Svensson, *J. Org. Chem.*, 2001, **66**, 4494.
33 P.-Y. Yeh, R. K. Kainthan, Y. Zou, M. Chiao and J. N. Kizhakkedathu, *Langmuir*, 2008, **24**, 4907.
34 D. G. Castner, K. Hinds and D. W. Grainger, *Langmuir*, 1996, **12**, 5083.
35 (*a*) J.-S. Park, A. N. Vo, D. Barriet, Y.-S. Shon and T. R. Lee, *Langmuir*, 2005, **21**, 2902; (*b*) Y.-S. Shon, R. Colorado, Jr., C. T. Williams, C. D. Bain and T. R. Lee, *Langmuir*, 2000, **16**, 541.

 This journal is © The Royal Society of Chemistry 2009

View Online

36 A. Chandekar, S. K. Sengupta, C. M. F. Barry, J. L. Mead and J. E. Whitten, *Langmuir*, 2006, **22**, 8071.
37 J.-S. Park, A. C. Smith and T. R. Lee, *Langmuir*, 2004, **20**, 5829.
38 The reviewer is appreciatively acknowledged for suggesting this effect.
39 G. G. Urquhart, J. W. Gates Jr. and R. Connor, *Org. Synth.*, 1955, **Coll. Vol. III**, 363.
40 W. P. Hall and E. E. Reid, *J. Am. Chem. Soc.*, 1943, **65**, 1466.
41 A. C. Templeton, M. J. Hostetler, C. T. Kraft and R. W. Murray, *J. Am. Chem. Soc.*, 1998, **120**, 1906.

Downloaded by Naval Research Laboratory - Washington on 09 November 2010
Published on 10 July 2009 on http://pubs.rsc.org | doi:10.1039/B906510P